Electromagnetic Model to Estimate the Vibrations of a Switched Reluctance Machine on the Basis of the Electric Power Supply

Benabdallah Mohammed Badreddine*

Abstract – The vibrations and noise origin in electric material is due to several coupled physical phenomena. The revolving electric machine complete modeling is complex; it does not allow simple parametric machine structure studies for various operation modes. This work presents a simple electromagnetic model which makes possible the machine principal parts flow estimation from flux density. Special interest is given in determining Switched Reluctance Machine (S.R.M) radial acceleration in accordance with the current supply.

Our focus will be only on the magnetic origin efforts that are dominating in the S.R.M. The efforts calculation versus the current is presented in the case of a machine with a linearized rate. These efforts are considered as a tangential force producing the torque and a radial force that generates no torque. The application is realized on a 6/4 low power S.R.M type (6 stator teeth and 4 teeth rotor). The mechanical response is substituted in a transfer function. The model takes account of the power supply of the machine, the relation between the current supply and the efforts as well as the vibratory response of the machine to these efforts. Finally, the model is validated by comparison with similar experimental results within the framework of the definite assumptions.

Keywords: Load modeling, Parameter, Traction power supply system

1. Introduction

The operation of the electric machines is always followed by vibrations of their structure and acoustic effects. The consequent deformations can involve deteriorations of the material and thus affect reliability. Moreover, vibrations of the external surface of the machine cause motion of the air and thus create an acoustic noise. This sound noise harms, by its intensity and especially by its frequencies, the user comfort. The evolution of the power electronics enhances interest of the Switched Reluctance Machine (S.R.M) because it maximizes its performances and confirms its use, but its impulse supply contains static inverters that accentuate the vibrations. Indeed, these converters deliver the harmonics signals able to excite one or more machine frequencies of unspecified power. The dynamic tests and the static allow the identification of the noise sources of the rotating machines and electromagnetics (electromagnetic strains, magnetostriction, Laplace forces). But, because of the multiplicity of the sound sources it is difficult to separate the mechanical and electromagnetic causes in normal operation. The electromagnetic causes are dominant and obtain a high level vibration with S.R.M and are clearly identifiable [1, 2]. These electromagnetic efforts deform the magnetic circuit and vary the pressure of the air on its surface thus generating the sound wave. The rotor, being more rigid and of radial surface lower than that of the stator, is less effective in causing air vibration, which moreover is confined inside the machine. The rotor thus produces a secondary power sound. Experiments show the strong dependence between the radial vibrations of the stator and the sound level of pressure statement close to the machine.

* Dept. of Electrical Engineering, University, Djilali Liabes, 22000, Sidi Belabbes, Algeria (e-mail : benabdallah22@yahoo.fr)
Received 21 January, 2007 ; Accepted 21 May, 2007

2. Magnetic Efforts

The deforming electromagnetic causes of the stator are:

- electromagnetic efforts on the magnetic circuit
- Laplace forces on the conductors

The efforts on the conductors are less than the magnetic efforts. The magnetostrictive deformations are much lower than the deformations due to these efforts in the case of the S.R.M. A different model exists for the computing these efforts. However, as long as the magnetic circuit remains without saturation, these models show that there are not big forces and that the surface forces are normal with the transition between two different magnetic mediums. The calculation model of the local efforts is based on the method of the virtual work applied to the case of a material linear that is homogeneous, isotropic and incompressible.

The local effort is then characterized by a pressure, Pn, which is normal to the transition in two materials, and directs the material of the highest permeability towards the material of the weakest permeability (Fig. 1):

$$P_n = \frac{1}{2}\left(B_n^2\left(\frac{1}{\mu_1}-\frac{1}{\mu_2}\right) - H_t^2(\mu_1-\mu_2)\right) \quad (1)$$

Where:
Pn: normal electromagnetic pressure (N.m2),
Bn: normal induction (T),
Ht: tangential field (A.m-1),
μ1 and μ2 permeabilities of Materials 1 and 2

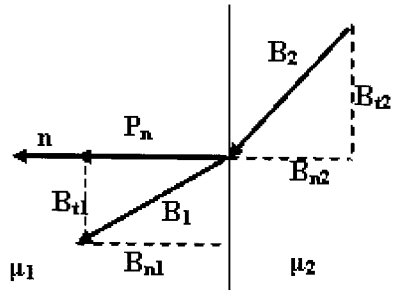

Fig. 1. Electromagnetic pressure at transition point of two materials transition

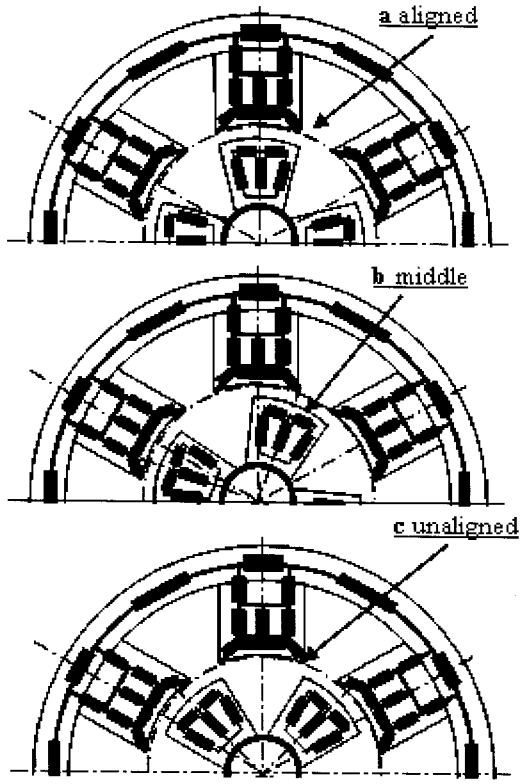

Fig. 2. Magnetic model for various rotor positions.
a. aligned **b.** middle **c.** unaligned

The magnetic stresses are obtained by calculating the flux density in the principal parts where we consider the machine supplied by a single-phase current with constant current I. These magnetic sizings are given for various positions of the rotor (Fig. 2).

The calculation of the magnetic pressure on the interior stator surface shows that these efforts are primarily localized on the teeth of the excited phase, and that the efforts tend to minimize the length of the field lines in the air (Figs. 3a, 3b, 3c) [3, 4]:

By rotative action of the rotor to bring a rotor tooth in the opposite direction (creation of torque);

By deformation of the stator (force not creating any torque).

3. Calculation of the radial and tangential Forces

The decomposition of rotation efforts and deformation brings the projection of these efforts in reference frame (radial-tangential) (Fig. 3d).

The quantitative study of the field of vectors formed by the radial and tangential pressures (and their effects) are not simple and examination will be limited only for their resultant Fr and Ft which have the same mechanical effects on the surface of the stator in order that the points of observation are suitably spaced from the points of load application (principle of Saint Venant). They are defined by:

$$F_r(\theta_m,I)_r = \int_S P_r.dS \ , \ F_t(\theta_m,I)_r = P_t.dS \quad (2)$$

Where:
Fr: radial force (N) ,
Pr: radial pressure (N.mm-2),
Ft: tangential force (N),
Pt: tangential pressure (N.mm-2),
θm: mechanical angle (rad),
I: phase current (A),
S being the surface defined by the contour of the excited tooth and the active length of the machine.

In the case of the rotor of the machine having 4 teeth, these forces have a periodicity of π/2. By calculating the torque created by the phase, Ns/q =2, and by considering the local pressure, the expression torque is [2]:

$$T = \frac{N_s}{q}\int_S \mathbf{P}_n \wedge \mathbf{r}dS \quad (3)$$

Where:
NS: the number of stator teeth,
q: phase number,
S: the surface of the tooth,
r: radius of the tooth (Fig. 3d).

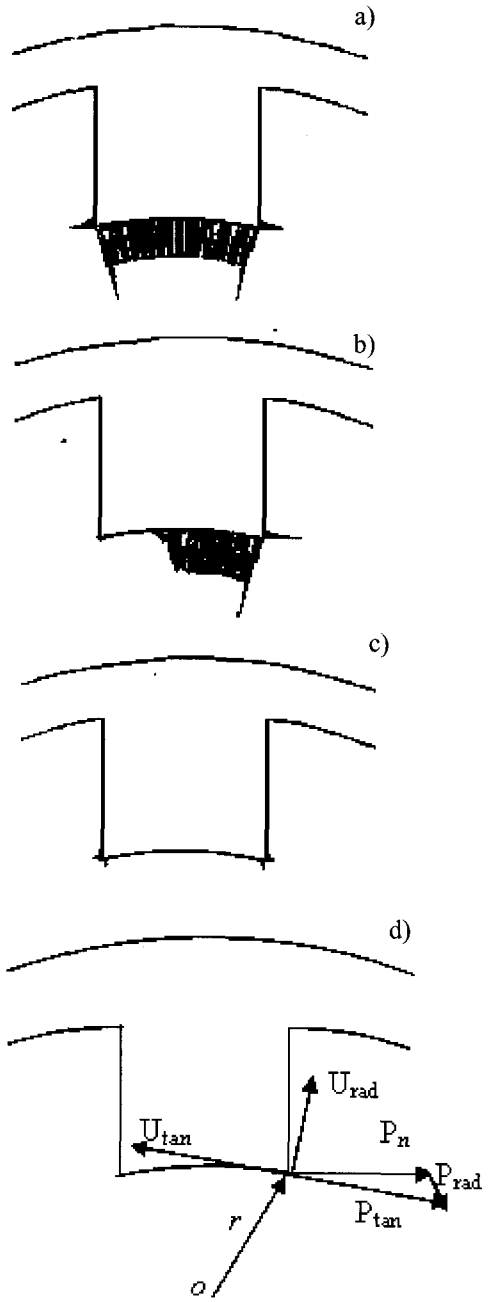

Fig. 3. Electromagnetic stress
a) aligned b) middle c) unaligned d) stress projection

The result of the tangential and radial forces calculation, with constant current, on only one of these teeth is represented in Fig. 4b according to the mechanical angle θm.

The result is compared with that obtained by the application of virtual work in a total way in linear mode (Fig. 4)

$$T = \frac{\partial W'_{em}(I,\theta_m)}{\theta_m} = \frac{1}{2} I^2 \frac{dL(\theta_m)}{d\theta_m} \qquad (4)$$

Where:

W' em: represents magnetic Co-energy,

L: is the phase inductance

The torque obtained in Fig. 4b is acceptable but since it is being obtained from the pressure, Pn, it must be done carefully [4, 5, 6]:

The calculation of Pn is carried out with the transition from two different materials. Otherwise, the numerical calculation by finite elements ensures that Figs. 3 a, b, c cannot maintain the continuity of Bn and HT simultaneously.

The torque is essentially created in the vicinity of the teeth ends where the numerical effects of the point are significant during the calculation of the magnetic sizes.

4. Forces with Variable Current

To determine the forces under normal operation it should be noted:

The magnetic field H and flux density B are proportional to the absorbed current for a given position and a linearized magnetic material (Fig. 4).

The torque T is proportional to the square of current I under normal operation,

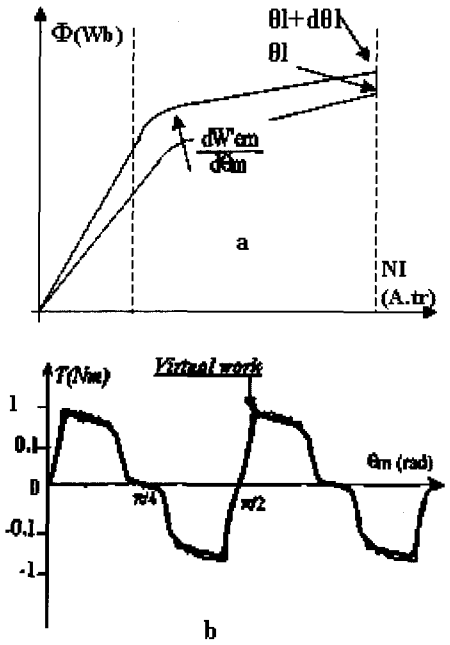

Fig. 4. Magnetic energy and torque

a) Magnetic energy and co-energy versus flux and Amperes turns.

b) Comparison of calculated torque by different methods with constant current versus mechanical position.

The magnetic pressure *Pn*, the radial forces *Fr*, and the tangential *Ft* are also to the square of current *I*:

$$T(I,\theta_m)=T_0(\theta_m)I^2 \quad F_r(I,\theta_m)=F_{r0}=(\theta_m)I^2 \quad (5)$$

Where:

To (θm) and *Fro(θm)* are the torque and the radial force respectively with *I = 1 A*

4.1 Radial acceleration.

The efforts are calculated before exciting the structure of the stator. The vibrations of this structure thus depend on the requests on the mechanical system implemented by a transfer function. The modal analysis allows the study of the complete mechanical system: the deformation in each point of the stator is then the sum of the deformations due to each mode of resonance at this point. These modes are characterized with:

Space deformation

Resonance frequency

Damping coefficient [2].

Our attention will be focused only on the point of the machine which vibrates more on the stator. This point, located in the axis of the tooth of the excited phase, is identifiable in the experiments. In this case, each mode can be characterized by a transfer function of the second order and the frequential relation between acceleration in this point and the radial force is given by Equation 5:

$$\frac{\gamma(p)}{F_r(p)}=H(p)=\sum A_i \frac{\frac{p^2}{\omega_i^2}}{1+2m_i\frac{p}{\omega_i}+\frac{p^2}{\omega_i^2}} \quad (6)$$

Where:

γ radial acceleration,

ω resonance pulsation of mode i,

mi, damping coefficient of mode i.

The frequential relation above is a total of strongly resonant high-pass functions. The direct measurement of this transfer function is not possible because the radial force Fr is not accessible.

The proportionality between this force and the square of the current (Fr(I,θm)=Fro(θm)I2)) permits to identify in experiments the coefficients of different high-pass [6].

The identification is carried out in conjunction where Fro (θm) is maximum. H(p) is then identified by:

$$H(p)=\frac{\gamma(p)}{F_r(p)}=\frac{1}{F_{r0}(\theta_m)}\frac{\gamma(p)}{L(i^2(t))} \quad (7)$$

where L represents the Laplace transform.

5. Complete modelization

The complete model consists of three blocks (Fig. 5):

- Electromagnetic block
- Mechanical block
- Electric block

The electric equation of the SRM phase is:

$$V(t)=Ri(t)+\Omega\frac{d\Phi(i,\theta_m)}{dt} \quad (8)$$

Where:

V (t) represents the terminal voltage,

Φ is the flux phase.

Assuming the rotational velocity constant, this equation becomes:

$$V(t)=Ri(t)+\Omega\frac{d[L(\theta m)i(\theta m)]}{d\theta m} \quad (9)$$

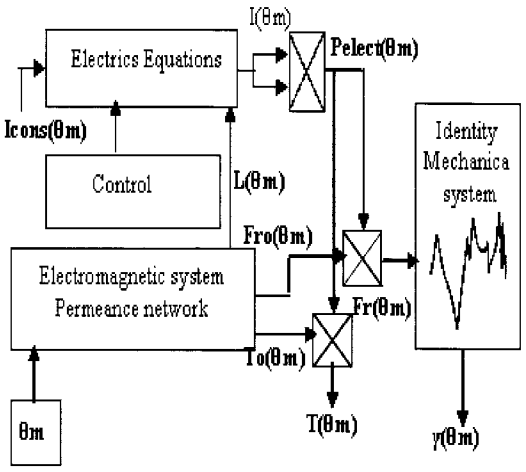

Fig. 5. Complete vibratory modelisation of the SRM

6. Validations

For a point in rotation operation, that is to say a power, the vibrations are evaluated by the model of the efforts and are compared with indirect measurements of the torque and the radial force [8, 9]. The studied SRM is three-phase of type 6/4 and its principal characteristics are 6 stator teeth and 4 rotor teeth with an external diameter of 63 mm, length of 60 mm, diameter of air-gap 34 mm, air-gap with the ray 0.4 mm, and 40 whorls per phase. The SRM is fed by a three-phase inverter with half asymmetrical bridges. This machine remains without magnetic saturation as long as the current does not exceed ten amps.

Constant current torque expression

The SRM is fed with constant current I and is driven by a motor with D.C. current at constant speed Ω. The rotational emf is:

$$E = \Omega . I \frac{dL(\theta_m)}{d\theta_m} \tag{10}$$

The torque is:

$$T = \frac{1}{2\Omega} EI \tag{11}$$

6.1 Expression of the radial force with constant current

The measurement of the torque can be done directly using a sensor, but the radial force requires an indirect measurement: the radial acceleration is measured under known exciting conditions to find the vibrating force. The idea is to supply the machine with constant current and to maintain a constant speed. But due to the mechanical response of the structure being a high-pass type, the radial acceleration is then of very low and unusable amplitude. To avoid this, the amplitude modulation principle of the radial force with a sinusoidal constant current Fro (θm) is introduced. The SRM is then fed by a sinusoidal current at frequency f1, such that the stator is not in resonance, and the machine is loaded at the speed Ω.

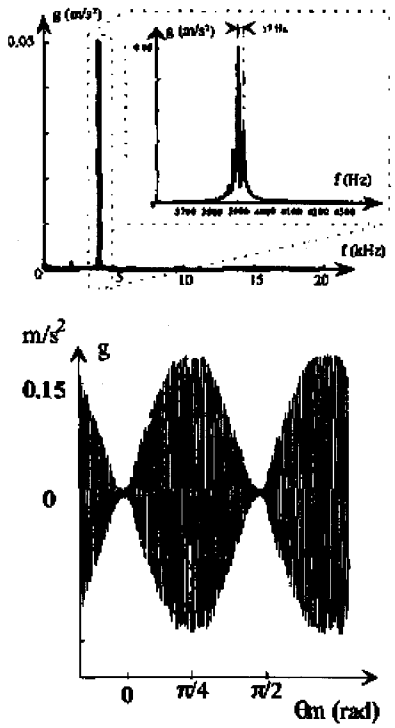

Fig. 6. Theoric and measured radial acceleration by differents representation

a) Frequency b) Mechanical position

Fig. 6 indicates the radial acceleration measured with a regulated current with an amplitude of 0.8 A. The rotational speed is 260 r.p.m. The radial force is according to the model and the amplitude modulation is Fro(θm).

Indeed: if

$$i(t) = I.\cos(2\pi f_1 t),$$

then

$$F_r(\theta_m, i(t)) = F_{r0}(\theta_m) i^2(t), \text{ so:}$$

$$F_r(\theta_m, i(t)) = \frac{F_{r0}(\theta_m) I^2}{2}(1 + \cos(2(2\pi f_1)t)) \tag{12}$$

This relation shows that the spectrum of the radial force is composed of two terms:

one centred around the frequency f = 0, representing the spectrum of

$$\frac{F_{r0}(\theta_m) I^2}{2},$$

one centered around the frequency $f = 2 f_1$, representing the same spectrum but shifted by $2f_1$; (3.7 kHz).

The position of these terms in the spectrum depends on the rotational frequency

$$N_r \frac{\Omega}{2\pi}.$$

These two terms are converted in the mechanical transfer function before being estimated on the radial acceleration spectrum [8, 9].

The first being at low frequency is eliminated by the filter of the mechanical transfer function.

The second is amplified by a constant profit (without being deformed) if the transfer function H(f) is considered constant in the spectral band of the second term. This helps to impose a low rotational speed and to choose the electric

frequency F so that the frequency 2f avoids resonance. In this situation, the measured radial force (represented in Fig. 7) is obtained by demodulating the radial acceleration measured and then by dividing it by the profit of the mechanical transfer function such as by the square of the amplitude of the current.

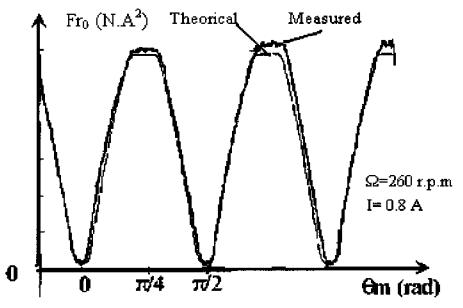

Fig. 7. Theoric and measured radial force

The observable difference on the regulation of the current is due to the method of simulation. It is without influence on acceleration in the audible frequency band.

The strong influence of commutations (face going up and especially descendant) of the current on the vibrations widen the spectral support of the efforts and thus excite resonances extremely far away from fundamental to 53 Hz (800 rev/min).

Remark: This validates the radial force qualitatively and not quantitatively because the knowledge of the mechanical transfer function H(f) is necessary and its determination requires initial radial force knowledge. The electromagnetic model of the radial force and the torque seems to slightly devaluate the efforts and their effects. Dissymmetry on the measured curves is explained by the losses, a weak hysteresis loop, and by the variation over one period number of revolutions.

6.2 Validation of the complete model under normal operation of the autopilot SRM

During the normal operation of the SRM, the current and the radial acceleration selected are compared under the same conditions in similar experiments in order to validate the complete model. The current is a crenel of 120° duration and of amplitude 6, 5A, the power supply has a voltage of 30 V, the load is involved at a speed of 800 r.p.m.

The controlled current is obtained using a MLI having a frequency of 40 kHz without effects on the sound Band (0-20 kHz).

This is observed Fig. 8 where the spectra of the measured and estimated radial acceleration are compared [10, 11].

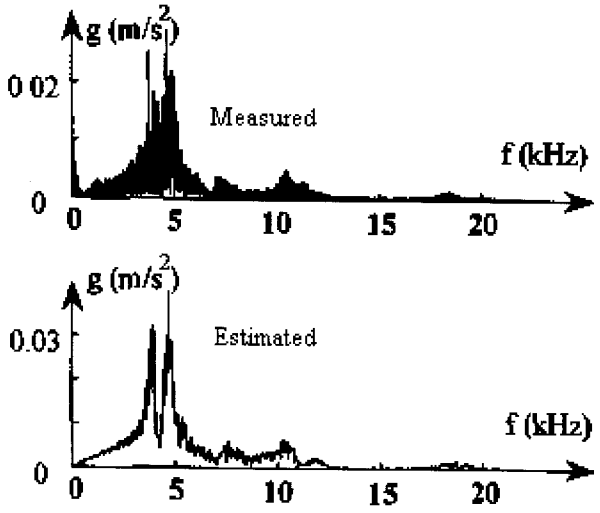

Fig. 8. Spectrum comparison of measured and estimated radial acceleration

Fig. 9 indicates that the SRM supplied with crenels of current produces significant vibrations at the time of the cut of the current because the radial force is then at maximum level and the fast descent of the current involves an intense relaxation of the radial force.

A first solution consists in slowing down the descent of the current by giving it a trapezoidal form. Fig. 10 demonstrates the crenel of current that is used as a reference of comparison and also two currents of trapezoidal form (currents 2 and 3 have angular duration of descent with the currents at 5° and 10°).

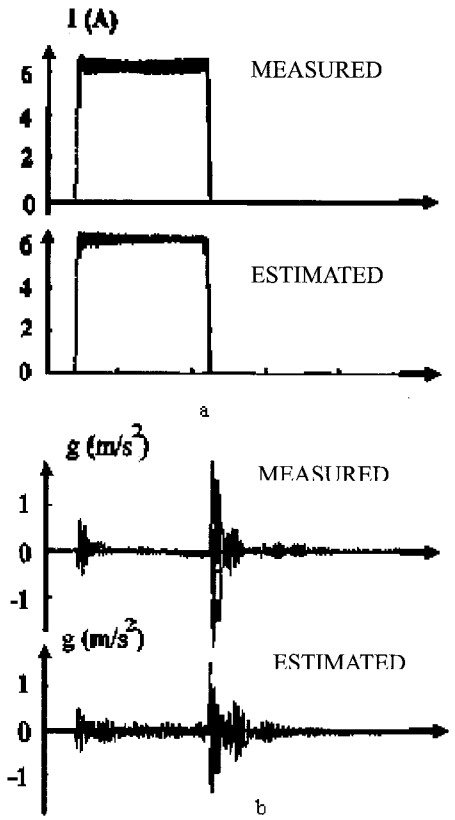

Fig. 9. Comparison
a) measured and estimated current
b) measured and estimated radial acceleration

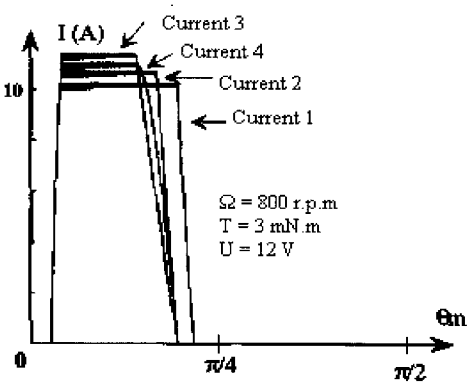

Fig. 10. Estimate current for different references

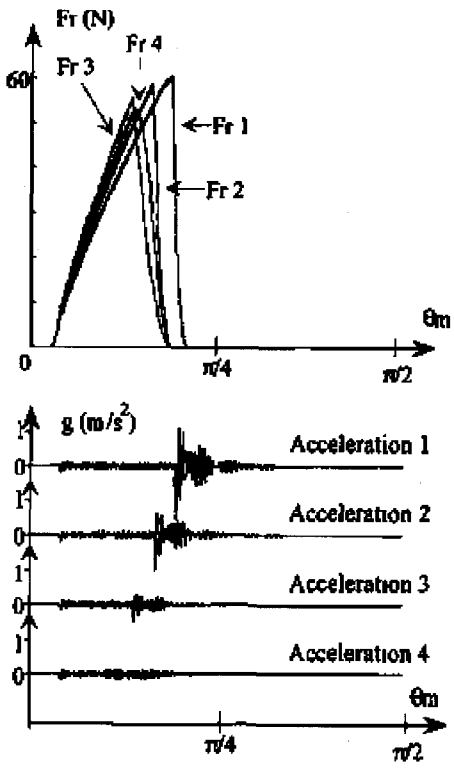

Fig. 11. Estimated radial forces and radial acceleration for different references

The currents represented have amplitudes that create the same average torque of 3 mN.m at 800 r.p.m.

The regulation of current is without effect in the band of the audio frequencies [12]. At constant torque, the amplitude of the trapezoid of the current is more significant, but the effect of the decrease of the current appears far from the conjunction. The amplitude of the radial force is finally decreased (Fig. 11) and the relaxation of the radial force is less intense as it is shown by the slopes of the obtained radial forces. However, to accentuate the reduction in the slope proves to be less effective and is limited by the quickly increasing maximum value of the current. Fig. 11 shows and compares the various radial accelerations obtained with two trapezoids of current. However, the change of the slope current generates vibrations. A softer form (current 4) will generate less vibration and be quieter [13].

The various shapes of current produce comparable Joule losses because the effective currents are similar. However on the level of the inverter, the constraints increase with the maximum value of the current. The attenuation of the effective value of acceleration for the current as compared to the crenel is theoretically about fifteen decibels.

The various shapes of current produce comparable Joule losses because the effective currents are similar. However, on the level of the inverter, the constraints increase with the maximum value of the current. The attenuation of the effective value of acceleration for the current as compared to the crenel is theoretically about fifteen decibels.

7. Conclusion

We presented a model of the radial vibrations of a S.R.M. under single-phase current operation in linearized magnetic mode. We described how the operation of power and the rotation to the rotor generate the efforts which excite the modes of the stator of resonance. This simple model is also used to define a discrete ordering and a certain regulation by setting instructions on the performances of the inverter-machine unit. At the time of the saturated mode, the distribution of the efforts is modified by:

- Volumic forces
- Surfacic forces are divided differently in amplitude and direction. The discretization of this part and the definition of a total radial force are conceivable for a similar study. The variation of other parameters, for example, the duration of conduction or the advance makes it possible to seek compromises between vibratory level and effective current or vibratory level and maximum current for a provided torque.

Finally, the symmetry of the efforts on the diametrical teeth support the modes of resonance which have the same space properties and attenuate the other modes which are not measurable.

References

[1] Multon B. Contribution to the optimization of the sets converters MRV and minimization of the factor of dimensioning. Doctoral Thesis ENS Cachan, Paris 1985.

[2] Multon B. Design and electronic power supply of the machines with MRVDS. ENS of Cachan Report March 17, 1994.

[3] Camus F, Gabsi M. Prediction of the vibrations of the stator of a variable reluctance machine according to the absorptive current. J Phys. III France 7 (1997) 387-404.

[4] Cameron O-F, Lang J-H- and Umans S-D. The Origin and Reduction of Acoustic Noise in DSMVR. Trans IEEE. Industry Applications 28 (November / December 1992) 1250-1255.

[5] Wu C-Y- and Pollock C. Time domain analysis of vibration and acoustic noise in the switched drive reluctance. International IEE Electrical Machines and Drives Conference (1993) pp. 558-563.

[6] Reyne G. Analyzes theoretical and experimental

vibratory phenomena of electromagnetic origin. PHD. National Polytechnic Institute of Grenoble (December 1987).

[7] Sedov L. Mechanics of the continuous mediums. Volumes II pp. 351-352. (Mir Edition).

[8] Besbes M. Contribution to the numerical modeling of the magneto elastic torqued phenomena. Application to the study of the vibrations of magnetic origin in the MRV, Thesis of Doctorate of the University Paris VI (June 14, 1995).

[9] Clenet S., Astier S., Lelvre Y. and Lajoie-Mazenc Mr. Method of measurement of the Eigen frequencies and the damping coefficients of a synchronous permanent magnet machine. J Phys. III France 4 (1994) 1431-1447.

[10] Cers P. Measurement and modeling of the transfer function entering the current and the vibrations of the stator of a machine to variable reluctance. Rapport of Training Course Engineer (LESiR, February 20, 1996).

[11] Colby R., Mottier F, and Miller T.J.E. Vibrations, modes, and acoustic noise in a 4 phases switched drive reluctance. IEEE Trans. Industry Applications (meeting 1995) pp. 441-447.

[12] Burnay G. The natural frequencies of vibrations and the critical engine. Failure speeds in the vibrations of torsion. Conference with the mechanical. Circle of studies University of Liege Belgium, 1943.

[13] Briguet R. Vibrations of the revolving machines and the Editions structures. Techniques and Documentations 1980.

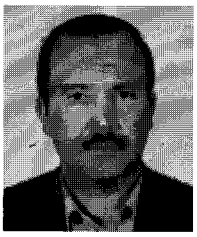

M Badreddine Benabdallah was born in Morocco in 1956. He studied at the University of Sciences and Technology in Oran (Algeria) and holds both an Engineer and Masters Degree in the Electrical Machines Field. For several years, he was part of the Technical Staff of many Algerian Enterprises and was involved in many National Projects. In 1984, he started his teaching experience as a Lecturer in the Electrical Engineering Department at the Djilali Liabes Sidi Bel Abbes University in Algeria. He is a Founding Member of the IRECOM laboratory (Interaction Network Converter Machines Lab.). Processes using design optimization based on experiments and data mining are his special fields of interest.